THE JOURNAL OF PHYSICAL CHEMISTRY Letters

Letter

pubs.acs.org/JPCL

Pushing the Photon Limit: Nanoantennas Increase Maximal Photon Stream and Total Photon Number

Emilie Wientjes,[†,‡] Jan Renger,[†,§] Richard Cogdell,[∥] and Niek F. van Hulst*[,†,⊥]

[†]ICFO – Institut de Ciencies Fotoniques, The Barcelona Institute of Science and Technology, 08860 Castelldefels, Barcelona, Spain
[‡]Laboratory of Biophysics, Wageningen University, 6703 HA Wageningen, The Netherlands
[§]Max Planck Institute for the Science of Light, D-91058 Erlangen, Germany
[∥]Glasgow Biomedical Research Building, Institute of Biomedical and Life Sciences, University of Glasgow, Glasgow G12 8QQ, U.K.
[⊥]ICREA – Institució Catalana de Recerca i Estudis Avançats, 08010 Barcelona, Spain

ABSTRACT: Nanoantennas are well-known for their effective role in fluorescence enhancement, both in excitation and emission. Enhancements of 3–4 orders of magnitude have been reported. Yet in practice, the photon emission is limited by saturation due to the time that a molecule spends in singlet and especially triplet excited states. The maximal photon stream restricts the attainable enhancement. Furthermore, the total number of photons emitted is limited by photobleaching. The limited brightness and observation time are a drawback for applications, especially in biology. Here we challenge this photon limit, showing that nanoantennas can actually increase both saturation intensity and photostability. So far, this limit-shifting role of nanoantennas has hardly been explored. Specifically, we demonstrate that single light-harvesting complexes, under saturating excitation conditions, show over a 50-fold antenna-enhanced photon emission stream, with 10-fold more total photons, up to 10^8 detected photons, before photobleaching. This work shows yet another facet of the great potential of nanoantennas in the world of single-molecule biology.

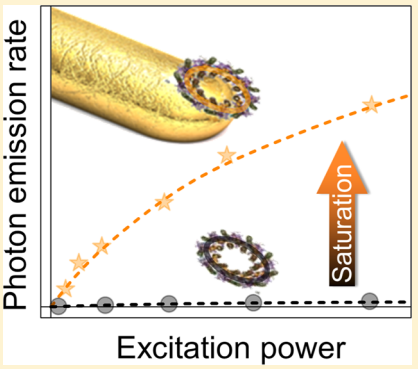

Plasmonic nanoantennas are metallic nanoparticles that are resonant at optical frequencies.[1] This leads to localization and concentration of the electromagnetic field into subdiffraction-limited volumes.[2−5] It is well-known that chromophores placed in the localized "hot spot" of such an antenna can show strong emission enhancement. This is usually mostly due to excitation enhancement. However, for low quantum yield emitters, enhancement of the radiative rate can also lead to emission enhancement. The combination of enhanced excitation and emission can lead to 500-fold brighter emission of single light-harvesting complexes[6] and even 1000-fold enhanced fluorescence of dye molecules.[7−9]

On the basis of the large enhancements, high quantum yields and short excited-state lifetimes of less than 100 ps[5,6,8] superemitters with 10^{10} counts per second could be expected. However, so far, this has not been observed. In practice, the maximal photon emission rate is not limited by the radiative rate to the ground state but by triplet states and photodissociation. The intersystem crossing (ISC) rate and bleach rate limit the photon count rate and number of emitted photons. Strangely enough, while the role of antennas to enhance the excitation and emission rates is widely appreciated, only a few single-molecule studies investigated the antenna enhancement of the typical number of emitted photons N; a 4-fold increase was reached by linking a chromophore to gold nanospheres,[10] and a 3-fold increase was found for fluorescent proteins in the presence of gold nanorods.[11] A large increase of the number of emitted photons was reported for single chromophores on gold sphere multimers,[12] but in this work, the characteristic total photon number N was not evaluated. Even more striking, it seems that the role of nanoantennas in enhancement of saturation levels has been largely overlooked.

In theory, a nanoantenna can enhance the emission saturation level of a molecule, as is demonstrated in the following equations. For a molecule excited with low power in the absence of a dark state, the detected photon count rate (PCR, s^{-1}) is given by eq 1, with κ the detection efficiency of the microscope, σ the molecular absorption cross section (cm^2), I_E the excitation intensity (W cm^{-2}), $h\nu$ the photon energy (J), k_r the radiative rate (s^{-1}), and k_{tot} the total decay rate (s^{-1}).

$$\mathrm{PCR} = \kappa \frac{\sigma}{h\nu} \frac{k_r}{k_{tot}} I_E \tag{1}$$

When the excitation power I_E is increased, and certainly with strong antenna enhancement, saturation effects start to occur and the equation changes into eq 2, with I_{Sat} as the saturation intensity[13,14]).

$$\mathrm{PCR} = \kappa \frac{\sigma}{h\nu} \frac{k_r}{k_{tot}} I_{Sat} \frac{I_E/I_{Sat}}{1 + (I_E/I_{Sat})} \tag{2}$$

Received: March 1, 2016
Accepted: April 15, 2016
Published: April 15, 2016

DOI: 10.1021/acs.jpclett.6b00491
J. Phys. Chem. Lett. 2016, 7, 1604−1609

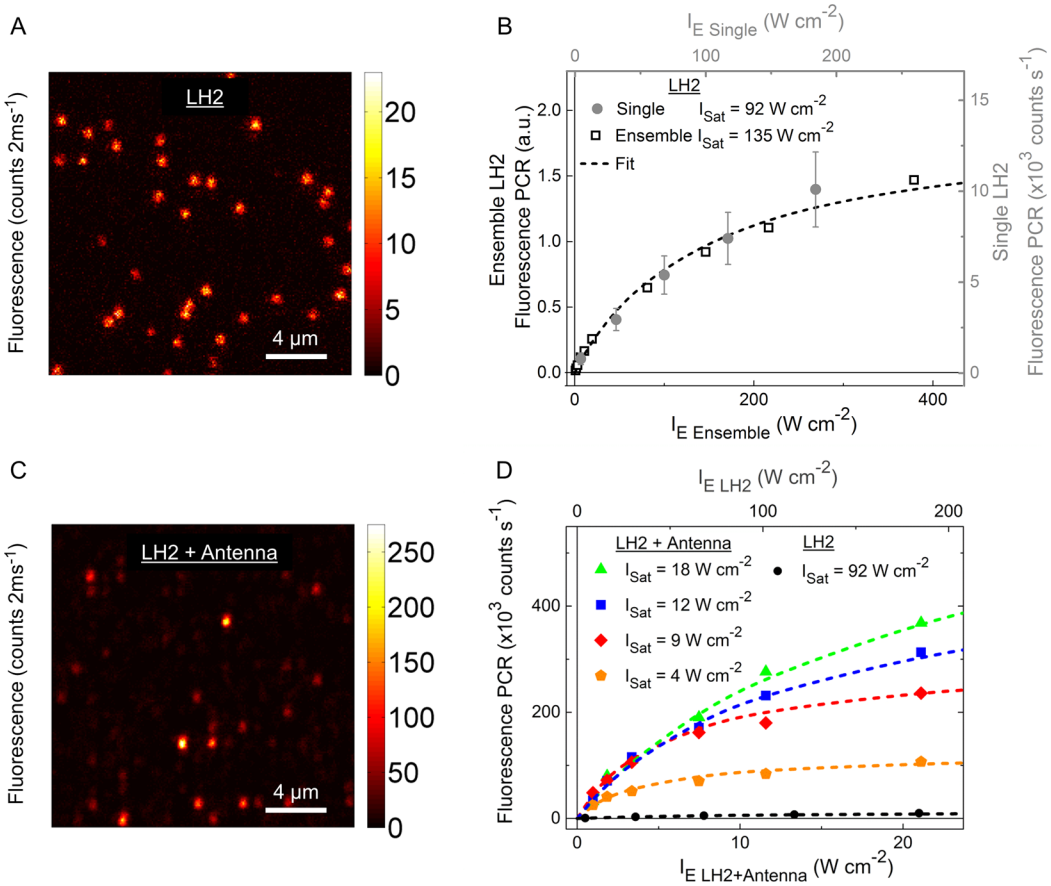

Figure 1. Antenna-enhanced photon count rate (PCR) at saturating excitation intensities. The PCR of LH2 in the absence and presence of a nanoantenna was followed as a function of the excitation power. Confocal fluorescence image of single LH2 complexes in PVA (A) or LH2 coated over an array of nanoantenna (C); excitation was with λ = 800 nm light at an intensity of 73 (A) or 4.3 W cm^{-2} (C). (C) Note that 400 nanoantennas, spaced 1 μm × 1 μm, are present in the scanned area. Only a few of them show bright fluorescence emission; those antennas have a single LH2 complex in their hot spot. (B,D) PCR of LH2 (B) and antenna-enhanced LH2 (D) emission as a function of the excitation power. The data were fitted with the equation PCR = $AI_E/[1 + (I_E/I_S)]$, giving the saturation intensity, and with $AI_E/2$, the PCR at saturation. The PCR at saturation was enhanced up to 53 times by the nanoantenna.

The saturation intensity is at the crossover between the linear and saturated regime, and at I_{Sat}, the PCR is half of the theoretical maximum reached at infinite excitation intensity. In the presence of a dark triplet state, with k_{ISC} the intersystem crossing rate from the singlet excited state to the triplet state (s^{-1}), $k_{tot} = k_r + k_{nr} + k_{ISC}$ (s^{-1}), and k_d the decay rate from the triplet state to the ground state (s^{-1}), the saturation intensity is given by eq 3.

$$I_{Sat} = \frac{h\nu}{\sigma}\frac{k_{tot}}{2 + (k_{ISC}/k_d)} \quad (3)$$

In the vicinity of a nanoantenna, k_{tot} is larger due to enhancement of k_r and k_{nr}; as a result, saturation will be reached at higher excitation intensities. Substitution of eq 3 in eq 2 gives the PCR at the saturation excitation intensity (PCR_{Sat}).

$$PCR_{Sat} = \frac{1}{2}\kappa\frac{k_r}{2 + (k_{ISC}/k_d)} \quad (4)$$

Note that the maximum PCR for $I_E \gg I_{Sat}$ is twice PCR_{Sat}. PCR_{Sat} scales linearly with the radiative rate k_r and thus with the Purcell factor for a molecule located in the hot spot of an antenna. Purcell factors as high a 600 at a wavelength of 1000 nm have been theoretically predicted for gold nanoantennas,[15] indicating that the saturation count rate can be substantially enhanced.

It has been shown that the emission of single LH2 complexes can be strongly enhanced with nanoantennas, profiting from both excitation and quantum yield enhancement.[6,16−18] Excitation enhancement is extremely useful for selective excitation of complexes present in the antenna hot spot, but it does not increase the maximum photon count rate. In this work, we investigate antenna enhancement of the PCR at saturating excitation intensities. The fluorescence intensity of single LH2 complexes in the absence and presence of gold nanorod antennas was studied as a function of the excitation intensity. To study single LH2s under control conditions, the complexes were diluted to 83 pM in an aqueous poly(vinyl alcohol) (PVA) solution and spin-casted over a glass coverslip (Figure 1A). The fluorescence as a function of the excitation intensity (linear polarized light, λ = 800 nm) is plotted in Figure 1B. The standard deviation is rather large, most likely due to variations in the orientations and environment of the individual LH2 complexes. Fitting the data shows that saturation occurs at around 92 W cm^{-2}, with a PCR_{Sat} of 6.4 × 10^3 counts s^{-1} and thus a maximal PCR for $I_E \gg I_{Sat}$ of 13 × 10^3 counts s^{-1}. In a second approach, a 4000-fold increased LH2 concentration was used to allow the excitation of a large

DOI: 10.1021/acs.jpclett.6b00491
J. Phys. Chem. Lett. 2016, 7, 1604−1609

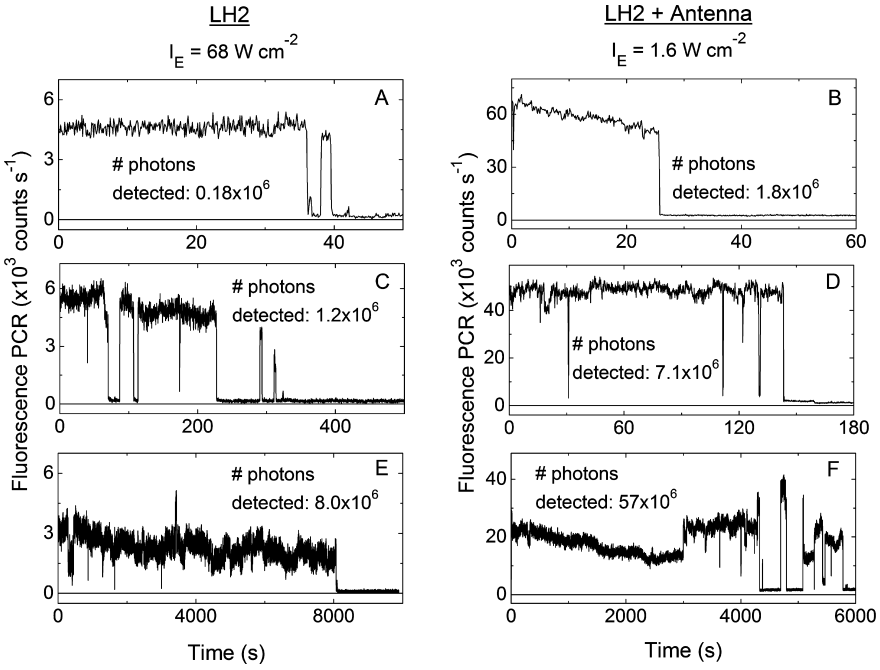

Figure 2. Single-molecule fluorescence of LH2. Examples of fluorescence time traces of LH2 in the absence (A,C,E) or presence (B,D,F) of a nanoantenna. The excitation intensity was 68 W cm^{-2} for LH2 and 43 times lower (1.6 W cm^{-2}) for LH2 + antenna. The on/off blinking shows that the fluorescence is emitted from a single LH2 complex. There is a large variation in photobleaching times, ranging from seconds (A,B) to hours (E,F). The number of detected photons is indicated for each trace.

number of complexes per diffraction-limited spot. In this ensemble experiment, variations between different areas were negligible. A higher saturation intensity was expected because the LH2 complexes were spread over the Gaussian intensity distribution of the excitation spot, while the single complexes were measured in the center of the spot at the highest intensity. This effect is partly compensated by the on/off blinking of single molecules. The off-switching rate is linearly dependent on the excitation intensity, while the on-switching rate is light-independent.[19] The off states are separated out in the single-molecule experiments, while they contribute to the ensemble measurement giving rise to an earlier apparent onset of saturation. The ensemble saturation occurred at 135 W cm^{-2}, in good agreement with the single-molecule measurements.

Next we focus on antenna-enhanced LH2 emission. LH2 complexes were diluted in a PVA solution to a concentration of 6.7 nM and spin-cast over e-beam lithography fabricated arrays of gold nanorod antennas, with dimensions of 50 nm × 60 nm × 160 nm, spaced 1 μm × 1 μm. Light of λ = 800 nm polarized along the long axis of the antenna was used for excitation. This light is resonant with the antenna and leads to enhanced excitation in the antenna hot spots. The LH2 concentration was chosen such that only in a fraction of the antenna was a single LH2 complex located in the hot spot, resulting in bright fluorescence emission[6] (Figure 1C). The single complexes were identified by the typical blinking behavior of their fluorescence (Figure 2), and their single photon emission behavior was confirmed by photon-antibunching, as we have shown before.[6] The fluorescence intensity as a function of the excitation power for a number of antenna-enhanced LH2 complexes is shown in Figure 1D. The saturation intensity ranges from 4 to 18 W cm^{-2}. Note that these are far-field intensities; the near-field intensities in the hot spot of the antenna can be 100-fold higher.[6] The PCR_{Sat} ranges from 61 × 10^3 to 340 × 10^3 counts s^{-1}, meaning that the antenna enhancement of PCR_{Sat} ranges from 10 to 53 times. PCR_{Sat} is linearly dependent on the radiative rate enhancement (eq 4), which is in turn strongly dependent on the orientation and distance of the chromophore dipole with respect to the antenna. On the basis of Finite Difference Time Domain simulations, a maximum radiative rate enhancement of 150-fold was predicted for an optimally orientated dipole (for LH2 emission at λ = 870 nm) located 5 nm from the antenna, while at 25 nm, the enhancement was decreased to 25-fold.[6] Thus, the experimentally observed enhancement of PCR_{Sat} is in the range expected from theory.

All single-molecule experiments are limited by the number of photons emitted before photobleaching (N). Increasing this number with the use of nanoantennas would be extremely valuable. In the simplest situation, photobleaching is a spontaneous decay process from the singlet excited state, occurring with rate k_b. In this case, the typical number of emitted photons (N) before bleaching is given by eq 5 and scales linearly with the Purcell factor.[10]

$$N = \frac{k_r}{k_b} \tag{5}$$

However, for a large number of organic chromophores, the bleaching process is more complex and, for instance, involves triplet states.[20−22] Under the relative high irradiance conditions used for single-molecule experiments, molecules in the first electronic excited singlet or triplet states, S_1 and T_1, may absorb a second photon and reach higher electronic states, S_n and T_n. These higher states are readily subjectable to photobleaching.[20] The number of emitted photons is no longer independent of the excitation intensity when bleaching occurs through such multiphoton processes. Instead, the highest number is reached at the lowest excitation power.[20,23] For such molecules, N will still increase with the Purcell factor as the molecules spend less

DOI: 10.1021/acs.jpclett.6b00491
J. Phys. Chem. Lett. 2016, 7, 1604−1609

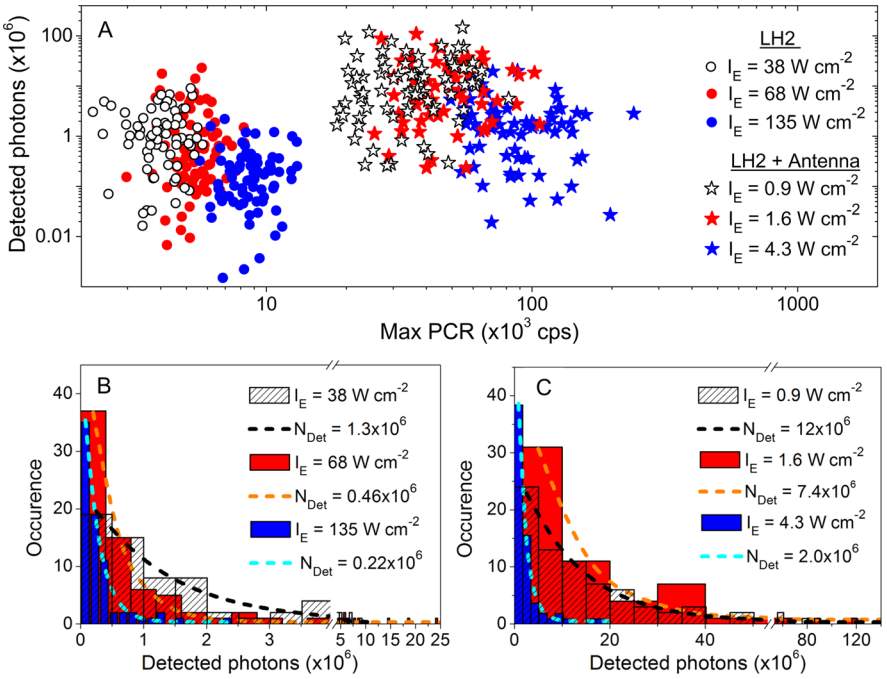

Figure 3. Ten times more photon at 10 times higher PCRs. A scatter plot of the number of photons detected from single LH2 complexes in the absence (circles) and presence (stars) of a nanoantenna against the maximal PCR of the complex. Three different excitation intensities were used as indicated in the legend; between 68 and 83 LH2 complexes were recorded per intensity. (B,C) Histograms showing the occurrence of the number of detected photons for single LH2 complexes in the absence (B) and presence (C) of the nanoantenna. Note the extended scale of detected photons for the histogram with the nanoantenna, on the right. The excitation intensity and photon detection number (N_{Det}, based on the single-exponential decay fit) are shown in the legend. For LH2, I_E = 38 W cm^{-2} measurements were stopped after a maximum of 50 min, while some complexes were still emitting. Those complexes only show up in the long tail of the histogram (B) and do not influence the exponential fit.

time in the excited state when k_r is enhanced, but the relation is no longer linear.

We investigated how the nanoantennas enhance the photostability of single LH2 complexes. Examples of fluorescence traces from single LH2 complexes are shown in Figure 2, with both no antenna (LH2) and antenna-enhanced (LH2 + antenna). The traces show the typical single-molecule on/off blinking and finally irreversible photobleaching. For some LH2 complexes, the PCR fluctuates between bright and dimmer states (Figure 2C,F). Such fluctuations have been seen before and were suggested to arise from different conformational states[24,25] or changes in the radiative rate of the LH2 complex and the formation of a photochemical product with a low probability to trap the excitation.[19] The LH2 complexes photobleach after seconds (Figure 2A,B), minutes (Figure 2C,D), or even hours (Figure 2E,F), with cases of up to 10^8 photons detected.

The total number of detected photons for each complex was plotted against the maximum photon count rate (Figure 3A), and photon number histograms were built (Figure 3B,C). Fitting of the histogram with an exponential decay function gives the statistical number of photons detected (N_{Det}), which relates to the bleach rate. Histograms were built for three excitation intensities, one close to the saturation intensity and two below. N_{Det} decreased with increasing excitation powers, both in the absence and in the presence of the antenna (Figure 3B,C), indicating that photobleaching of the LH2 complexes occurs through a multiphoton process.[20,23] In Figure 4, N_{Det} is plotted against PCR averaged for all of the complexes measured with the same excitation intensity. Higher PCRs come at the cost of a decreased N_{Det}. However, in the presence of the antenna, both the PCR and N_{Det} are approximately 10 times

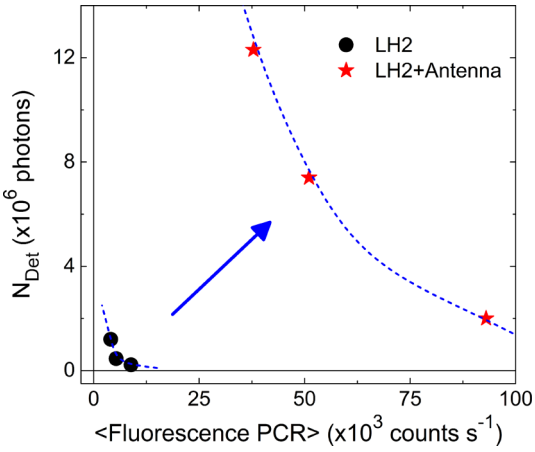

Figure 4. Number of detected (N_{Det}) photons as a function of the average PCRs for LH2 in the absence and presence of the antenna. The dashed line is a guide line for the eye. In the presence of the nanoantenna, both N_{Det} and the PCR are 10-fold higher at about 40-times lower excitation powers.

higher compared to the control situation. As such, a single molecule can be measured for the same amount of time with 10-fold higher PCR, allowing processes to be monitored at a 10-fold higher sampling rate.

We did not measure the antenna-enhanced N_{Det} at the same low PCRs (4×10^3 to 9×10^3 counts s^{-1}) as assessed for LH2 without antenna. However, roughly extrapolating the data indicates that under these conditions, N_{Det} would be about 2 orders of magnitude larger. This provides the ideal situation to follow single molecules for a very long time.

DOI: 10.1021/acs.jpclett.6b00491
J. Phys. Chem. Lett. 2016, 7, 1604−1609

Single-molecule techniques have found applications in a wide range of life science research fields, including DNA sequencing,[26] super-resolution imaging,[27,28] and photosynthesis.[29−35] However, the maximal number of photons that a single complex can emit per second is restricted by its intrinsic properties. In addition, the total number of photons that a single complex can emit, especially at physiologically relevant temperatures, is limited. This hinders the observation of fast changes and fluctuations in the complex and sets the boundary for the total measurement time. Clearly, a general method that alleviates these restrictions would be valuable. Here we demonstrate an over 50-fold nanoantenna enhancement of the maximum photon count rate from a single light-harvesting complex (LH2). The total number of photons that a single LH2 complex emits was shown to depend on the excitation intensity. The average photon count rate and the total number of detected photons were simultaneously enhanced 10 times by the nanoantenna at approximately 40-times lower laser intensities. These intense enhancements show the great potential of nanoantennas for photosynthesis research in particular and single-molecule biology in general.

EXPERIMENTAL METHODS

Sample Preparation. Gold nanorods (50 nm × 60 nm × 160 nm) were fabricated on a glass coverslip with a 50 nm Au layer and a 1 nm titanium adhesion layer by negative-tone electron-beam lithography in combination with reactive-ion etching. LH2 was purified from *Rhodopseudomonas acidophila* (strain 10 050), as described previously.[36] This cylindrical complex coordinates 9 bacteriochlorophylls that absorb at λ = 800 nm and 18 bacteriochlorophylls that absorb at λ = 860 nm; the latter shows an emission band at around λ = 870 nm.[37,38] LH2 was diluted in an aqueous PVA solution (10 mM tricine pH 8.0, 0.03% α-dodecyl-*n*-maltoside, 0.45% PVA: Mowiol 20-98, Mw 125 kDa, Sigma-Aldrich) and spin-casted over a glass coverslip with or without a nanoantenna array at 3000 rpm for 30 s.

Confocal Microscopy. Microscopy was performed using a commercial time-resolved confocal microscope (Micro Time 200, PicoQuant, Germany). The excitation was with linearly polarized pulsed light at λ = 800 nm (Titanium−Sapphire pulsed laser, Coherent-Mira), with a repetition rate of 76 MHz. A high numerical aperture (1.46, 100×, Zeiss) oil immersion objective mounted on an inverted microscope (Olympus) was used for both excitation and collection. The fluorescence light was separated from the excitation light using a dichroic mirror and long-pass filters (λ = 835 nm + 850 nm) and detected by an avalanche photodiode (MPD, Micro Photon Devices).

AUTHOR INFORMATION

Corresponding Author

*E-mail: Niek.vanHulst@ICFO.eu.

Notes

The authors declare no competing financial interest.

ACKNOWLEDGMENTS

This research was funded by the European Commission (ERC Adv. Grant 247330-NanoAntennas and ERC Adv. Grant 670949-LightNet), Spanish MINECO (Project FIS2012-35527 cofunded by FEDER; Network FIS2014-55563-REDC and Severo Ochoa Programme for Centres of Excellence in R&D SEV-2015-0522), the Catalan AGAUR (2014 SGR01540), and Fundació CELLEX (Barcelona). R.C. thanks the Biotechnology and Biological Sciences Research Council (BBSRC) for financial support. E.W. acknowledges financial support from the Marie-Curie International Fellowship COFUND and ICFOnest program and from an individual Marie Sklodowska-Curie fellowship 655542.

REFERENCES

(1) Novotny, L.; van Hulst, N. Antennas for Light. *Nat. Photonics* **2011**, *5*, 83−90.
(2) Fromm, D. P.; Sundaramurthy, A.; Schuck, P. J.; Kino, G.; Moerner, W. E. Gap-Dependent Optical Coupling of Single "Bowtie" Nanoantennas Resonant in the Visible. *Nano Lett.* **2004**, *4*, 957−961.
(3) Mühlschlegel, P.; Eisler, H. J.; Martin, O. J.; Hecht, B.; Pohl, D. W. Resonant Optical Antennas. *Science* **2005**, *308*, 1607−1609.
(4) Taminiau, T. H.; Moerland, R. J.; Segerink, F. B.; Kuipers, L.; van Hulst, N. F. Lambda/4 Resonance of an Optical Monopole Antenna Probed by Single Molecule Fluorescence. *Nano Lett.* **2007**, *7*, 28−33.
(5) Punj, D.; Mivelle, M.; Moparthi, S. B.; van Zanten, T. S.; Rigneault, H.; van Hulst, N. F.; Garcia-Parajo, M. F.; Wenger, J. A Plasmonic 'Antenna-in-Box' Platform for Enhanced Single-Molecule Analysis at Micromolar Concentrations. *Nat. Nanotechnol.* **2013**, *8*, 512−516.
(6) Wientjes, E.; Renger, J.; Curto, A. G.; Cogdell, R.; van Hulst, N. F. Strong Antenna-Enhanced Fluorescence of a Single Light-Harvesting Complex Shows Photon Antibunching. *Nat. Commun.* **2014**, *5*, 1−7.
(7) Yuan, H.; Khatua, S.; Zijlstra, P.; Yorulmaz, M.; Orrit, M. Thousand-Fold Enhancement of Single-Molecule Fluorescence near a Single Gold Nanorod. *Angew. Chem., Int. Ed.* **2013**, *52*, 1217−21.
(8) Kinkhabwala, A.; Yu, Z. F.; Fan, S. H.; Avlasevich, Y.; Mullen, K.; Moerner, W. E. Large Single-Molecule Fluorescence Enhancements Produced by a Bowtie Nanoantenna. *Nat. Photonics* **2009**, *3*, 654−657.
(9) Khatua, S.; Paulo, P. M.; Yuan, H.; Gupta, A.; Zijlstra, P.; Orrit, M. Resonant Plasmonic Enhancement of Single-Molecule Fluorescence by Individual Gold Nanorods. *ACS Nano* **2014**, *8*, 4440−9.
(10) Pellegrotti, J. V.; Acuna, G. P.; Puchkova, A.; Holzmeister, P.; Gietl, A.; Lalkens, B.; Stefani, F. D.; Tinnefeld, P. Controlled Reduction of Photobleaching in DNA Origami-Gold Nanoparticle Hybrids. *Nano Lett.* **2014**, *14*, 2831−2836.
(11) Donehue, J. E.; Wertz, E.; Talicska, C. N.; Biteen, J. S. Plasmon-Enhanced Brightness and Photostability from Single Fluorescent Proteins Coupled to Gold Nanorods. *J. Phys. Chem. C* **2014**, *118*, 15027−15035.
(12) Cang, H.; Liu, Y. M.; Wang, Y.; Yin, X. B.; Zhang, X. Giant Suppression of Photobleaching for Single Molecule Detection Via the Purcell Effect. *Nano Lett.* **2013**, *13*, 5949−5953.
(13) de Vries, H.; Wiersma, D. A. Photophysical and Photochemical Molecular Hole Burning Theory. *J. Chem. Phys.* **1980**, *72*, 1851−1863.
(14) Ambrose, W. P.; Basche, T.; Moerner, W. E. Detection and Spectroscopy of Single Pentacene Molecules in a Para-Terphenyl Crystal by Means of Fluorescence Excitation. *J. Chem. Phys.* **1991**, *95*, 7150−7163.
(15) Mohammadi, A.; Sandoghdar, V.; Agio, M. Gold Nanorods and Nanospheroids for Enhancing Spontaneous Emission. *New J. Phys.* **2008**, *10*, 105015.
(16) Bujak, L.; Olejnik, M.; Brotosudarmo, T. H.; Schmidt, M. K.; Czechowski, N.; Piatkowski, D.; Aizpurua, J.; Cogdell, R. J.; Heiss, W.; Mackowski, S. Polarization Control of Metal-Enhanced Fluorescence in Hybrid Assemblies of Photosynthetic Complexes and Gold Nanorods. *Phys. Chem. Chem. Phys.* **2014**, *16*, 9015−22.
(17) Wientjes, E.; Renger, J.; Curto, A. G.; Cogdell, R.; van Hulst, N. F. Nanoantenna Enhanced Emission of Light-Harvesting Complex 2: The Role of Resonance, Polarization, and Radiative and Non-Radiative Rates. *Phys. Chem. Chem. Phys.* **2014**, *16*, 24739−46.
(18) Beyer, S. R.; Ullrich, S.; Kudera, S.; Gardiner, A. T.; Cogdell, R. J.; Kohler, J. Hybrid Nanostructures for Enhanced Light-Harvesting: Plasmon Induced Increase in Fluorescence from Individual Photo-

DOI: 10.1021/acs.jpclett.6b00491
J. Phys. Chem. Lett. 2016, 7, 1604−1609

synthetic Pigment-Protein Complexes. *Nano Lett.* **2011**, *11*, 4897−901.
(19) Bopp, M. A.; Jia, Y. W.; Li, L. Q.; Cogdell, R. J.; Hochstrasser, R. M. Fluorescence and Photobleaching Dynamics of Single Light-Harvesting Complexes. *Proc. Natl. Acad. Sci. U. S. A.* **1997**, *94*, 10630−10635.
(20) Eggeling, C.; Widengren, J.; Rigler, R.; Seidel, C. A. M. Photobleaching of Fluorescent Dyes under Conditions Used for Single-Molecule Detection: Evidence of Two-Step Photolysis. *Anal. Chem.* **1998**, *70*, 2651−2659.
(21) Wennmalm, S.; Rigler, R. On Death Numbers and Survival Times of Single Dye Molecules. *J. Phys. Chem. B* **1999**, *103*, 2516−2519.
(22) Song, L. L.; Varma, C. A. G. O.; Verhoeven, J. W.; Tanke, H. J. Influence of the Triplet Excited State on the Photobleaching Kinetics of Fluorescein in Microscopy. *Biophys. J.* **1996**, *70*, 2959−2968.
(23) Deschenes, L. A.; Vanden Bout, D. A. Single Molecule Photobleaching: Increasing Photon Yield and Survival Time through Suppression of Two-Step Photolysis. *Chem. Phys. Lett.* **2002**, *365*, 387−395.
(24) Schlau-Cohen, G. S.; Wang, Q.; Southall, J.; Cogdell, R. J.; Moerner, W. E. Single-Molecule Spectroscopy Reveals Photosynthetic Lh2 Complexes Switch between Emissive States. *Proc. Natl. Acad. Sci. U. S. A.* **2013**, *110*, 10899−903.
(25) Schorner, M.; Beyer, S. R.; Southall, J.; Cogdell, R. J.; Kohler, J. Multi-Level, Multi Time-Scale Fluorescence Intermittency of Photosynthetic Lh2 Complexes: A Precursor of Non-Photochemical Quenching? *J. Phys. Chem. B* **2015**, *119*, 13958−63.
(26) Eid, J.; Fehr, A.; Gray, J.; Luong, K.; Lyle, J.; Otto, G.; Peluso, P.; Rank, D.; Baybayan, P.; Bettman, B.; et al. Real-Time DNA Sequencing from Single Polymerase Molecules. *Science* **2009**, *323*, 133−138.
(27) van de Linde, S.; Heilemann, M.; Sauer, M. Live-Cell Super-Resolution Imaging with Synthetic Fluorophores. *Annu. Rev. Phys. Chem.* **2012**, *63*, 519−540.
(28) Huang, B.; Babcock, H.; Zhuang, X. W. Breaking the Diffraction Barrier: Super-Resolution Imaging of Cells. *Cell* **2010**, *143*, 1047−1058.
(29) van Oijen, A. M.; Ketelaars, M.; Kohler, J.; Aartsma, T. J.; Schmidt, J. Unraveling the Electronic Structure of Individual Photosynthetic Pigment-Protein Complexes. *Science* **1999**, *285*, 400−402.
(30) Hofmann, C.; Ketelaars, M.; Matsushita, M.; Michel, H.; Aartsma, T. J.; Kohler, J. Single-Molecule Study of the Electronic Couplings in a Circular Array of Molecules: Light-Harvesting-2 Complex from Rhodospirillum Molischianum. *Phys. Rev. Lett.* **2003**, *90*, 1−4.
(31) Hofmann, C.; Aartsma, T. J.; Michel, H.; Kohler, J. Spectral Dynamics in the B800 Band of Lh2 from Rhodospirillum Molischianum: A Single-Molecule Study. *New J. Phys.* **2004**, *6*, 8.
(32) Kruger, T. P. J.; Wientjes, E.; Croce, R.; van Grondelle, R. Conformational Switching Explains the Intrinsic Multifunctionality of Plant Light-Harvesting Complexes. *Proc. Natl. Acad. Sci. U. S. A.* **2011**, *108*, 13516−13521.
(33) Tietz, C.; Jelezko, F.; Gerken, U.; Schuler, S.; Schubert, A.; Rogl, H.; Wrachtrup, J. Single Molecule Spectroscopy on the Light-Harvesting Complex Ii of Higher Plants. *Biophys. J.* **2001**, *81*, 556−562.
(34) Brecht, M.; Radics, V.; Nieder, J. B.; Bittl, R. Protein Dynamics-Induced Variation of Excitation Energy Transfer Pathways. *Proc. Natl. Acad. Sci. U. S. A.* **2009**, *106*, 11857−11861.
(35) Hildner, R.; Brinks, D.; Nieder, J. B.; Cogdell, R. J.; van Hulst, N. F. Quantum Coherent Energy Transfer over Varying Pathways in Single Light-Harvesting Complexes. *Science* **2013**, *340*, 1448−1451.
(36) Gardiner, A. T.; Takaichi, S.; Cogdell, R. J. The Effect of Changes in Light Intensity and Temperature on the Peripheral Antenna of Rhodopseudomonas Acidophila. *Biochem. Soc. Trans.* **1993**, *21*, 6S.
(37) Cogdell, R. J.; Gall, A.; Köhler, J. The Architecture and Function of the Light-Harvesting Apparatus of Purple Bacteria: From Single Molecules to in Vivo Membranes. *Q. Rev. Biophys.* **2006**, *39*, 227−324.
(38) McDermott, G.; Prince, S. M.; Freer, A. A.; Hawthornthwaite-Lawless, A. M.; Papiz, M. Z.; Cogdell, R. J.; Isaacs, N. W. Crystal-Structure of an Integral Membrane Light-Harvesting Complex from Photosynthetic Bacteria. *Nature* **1995**, *374*, 517−521.

DOI: 10.1021/acs.jpclett.6b00491
J. Phys. Chem. Lett. 2016, 7, 1604−1609